

## Bio-inspired multifunctional metallic glass

Yaxu He<sup>1</sup>, Yun Peng<sup>1</sup>, Zhou Li<sup>1</sup>, Jiang Ma<sup>2</sup>, Xiyao Zhang<sup>1</sup>, Kesong Liu<sup>1\*</sup>,  
Weihua Wang<sup>2\*</sup> & Lei Jiang<sup>1,3</sup>

<sup>1</sup>Key Laboratory of Bio-Inspired Smart Interfacial Science and Technology of Ministry of Education; Beijing Key Laboratory of Bio-Inspired Energy Materials and Devices; School of Chemistry and Environment, Beihang University, Beijing 100191, China

<sup>2</sup>Institute of Physics, Chinese Academy of Sciences, Beijing 100190, China

<sup>3</sup>Beijing National Laboratory for Molecular Sciences; Key Laboratory of Organic Solids; Institute of Chemistry, Chinese Academy of Sciences, Beijing 100190, China

Received June 10, 2015; accepted June 24, 2015; published online November 3, 2015

As a novel class of metallic materials, bulk metallic glasses (BMGs) have attracted a great deal of attention owing to their technological promise for practical engineering applications. In nature, biological materials exhibit inherent multifunctional integration, which provides some inspiration for scientists and engineers to construct multifunctional artificial materials. In this contribution, inspired by superhydrophobic self-cleaning lotus leaves, multifunctional bulk metallic glasses (BMG) materials have been fabricated through the thermoplastic forming-based process followed by the SiO<sub>2</sub>/soot deposition. To mimic the micro-scale papillae of the lotus leaf, the BMG micropillar with a hemispherical top was first fabricated using micro-patterned silicon templates based on thermoplastic forming. The deposited randomly distributed SiO<sub>2</sub>/soot nanostructures covered on BMG micropillars are similar to the branch-like nanostructures on papillae of the lotus leaf. Micro-nanoscale hierarchical structures endow BMG replica with superhydrophobicity, a low adhesion towards water, and self-cleaning, similar to the natural lotus leaf. Furthermore, on the basis of the observation of the morphology of BMG replica in the Si mould, the formation mechanism of BMG replica was proposed in this work. The BMG materials with multifunction integration would extend their practical engineering applications and we expect this method could be widely adopted for the fabrication of other multifunctional BMG surfaces.

**biological materials, bio-inspired materials, multifunction**

**Citation:** He YX, Peng Y, Li Z, Ma J, Zhang XY, Liu KS, Wang WH, Jiang L. Bio-inspired multifunctional metallic glass. *Sci China Chem*, 2016, 59: 271–276, doi: 10.1007/s11426-015-5496-5

### 1 Introduction

Bulk metallic glasses (BMGs), a novel class of metallic materials, are regarded as one of the most important potential engineering materials. Since the first report of metallic glass by Klement *et al.* [1] in 1960, a large number of BMGs with excellent glass-forming ability have been fabricated using different synthesis strategies. These BMGs

exhibit unique thermal, mechanical, magnetic, and other properties. In recent years, BMGs have attracted much attention because of their scientific importance and technological promise in fundamental research and practical applications [2–6]. One of unique features of BMGs is the temperature-dependent mechanical behavior. Recently, a number of processing methods have been developed to process BMGs like plastics for the generation of complex surface structures with well-defined geometry and shape on length scales ranging from nano, micro, to macro [7–10]. The creation of special surface structures provides an

\*Corresponding authors (email: liuks@buaa.edu.cn; whw@aphy.iphy.ac.cn)

avenue to construct multifunctional BMGs through the surface modification, which could significantly extend their practical applications.

After millions of years of evolution, biological materials are typically multifunctional [11–16]. Creating multifunctional materials is an eternal goal for scientists. The progress in advanced materials often relies on the biological solutions provided by the nature around us. Optimized biological solutions provide inspiration for scientists and engineers to design and fabricate multifunctional materials. Surface wettability of a solid material by a liquid is a classical and important aspect of surface science, which is governed by the surface chemical composition and surface geometrical structures. In nature, a wide variety of biological materials exhibit excellent surface wettability, such as lotus leaves, mosquito eyes, water strider legs, insect wings, gecko feet, desert beetle, and spider silks [17–24]. Inspired by nature, a great number of multifunctional materials with special wettability have been fabricated through increasing the surface roughness and lowering the surface energy [25–32]. Among the variety of biomaterials with special wettability, the lotus leaf (*Nelumbo nucifera*), better known as the water lily, is one of most promising. It has been demonstrated that the lotus leaf surfaces possess micro-nanoscale hierarchical structures in the form of micro-papillae covered by branch-like nanostructures. The cooperation of surface multiscale structures and hydrophobic epicuticular waxes confers a high water contact angle and a small sliding angle. Water droplets on the lotus leaf surface are almost spherical and can roll freely in all directions and then pick up dirt particles, exhibiting superhydrophobic, low-adhesion, and self-cleaning properties. A very high static water contact angle and a very low sliding angle are essential for the final formation superhydrophobicity-induced self-cleaning.

Here, inspired by the superhydrophobic self-cleaning lotus leaf, multifunctional BMGs were fabricated by combining the thermoplastic forming-based micro-fabrication method with the post-deposition. The resultant BMG surfaces possessed microscale pillars with a hemispherical top covered by post-deposited randomly distributed nanostructures, which is similar to the lotus leaf with micro-papillae covered by branch-like nanostructures. Multiscale surface structures endow the BMG replica with lotus leaf-like low adhesive superhydrophobicity and self-cleaning. Wettability is a fundamental property of a solid surface, which plays an important role in determining the performance of the bulk material. The bio-inspired construction of multifunctional BMGs with special wettability is important for both basic research and for extending the application of BMGs. In combination with low adhesive superhydrophobicity, self-cleaning, high strength and elasticity, good corrosion resistance, and biocompatibility, BMGs could have prospective applications in nanofabrication, catalysis, electrochemical reactor, small-scale

devices, medical implants, and other potential fields.

## 2 Experimental

### 2.1 Materials

Silicon wafer (Grimm Semiconductor Materials Co. Ltd, China), tetraethoxysilane (TEOS, Sigma-Aldrich, USA), ammonia (Xilong Chemical Co. Ltd., China), and ethanol (Xilong Chemical Co. Ltd., China) were used as received. The  $\text{Ce}_{65}\text{Al}_{10}\text{Cu}_{20}\text{Co}_5$  BMG was prepared by sucking the melt into copper mold [33]. Micro-patterned silicon wafers were prepared by photolithography and an inductively coupled plasma deep-etching technique. Contact lithographic masks were constructed by Microelectronics R&D Center, the Chinese Academy of Sciences. A Karl Suss MA6 (Germany) instrument was used to transfer the patterns of masks onto silicon wafers by a photolithographic method. A deep-etching process was completed using an STS ICP ASE (UK) instrument. The size of the square silicon micro-pit is  $20\ \mu\text{m}$  (length) $\times$  $20\ \mu\text{m}$  (width) $\times$   $28\text{--}30\ \mu\text{m}$  (depth). The spacing between the nearest micro-pits is  $9\ \mu\text{m}$ .

### 2.2 Preparation of multifunctional BMGs

Si moulds were positioned on the platform of the setup and were heated to  $110\text{--}130\ ^\circ\text{C}$ . A piece of BMG was placed on the heated Si mould for 20 s to reach the equilibrium temperature. In order to fill the cavity of Si moulds, the compressive pressure was applied on the BMG using a universal testing machine with the moving rate of  $0.180\ \text{mm/min}$ . The applied pressure was precisely kept constant at 30 MPa. An ordered array of BMG micro-pillars could be formed after dissolving the Si mould in a KOH solution by further heating. The resultant BMG replica was ultrasonically cleaned for several minutes in ethanol solution to eliminate the oil stains on its surface. In order to fabricate lotus leaves-like low adhesive superhydrophobic surfaces, the BMG replica with micro-pillars was placed in the vacuum desiccator together with two open glass vessels containing TEOS and aqueous ammonia solution, respectively. Silica can be formed on the BMG replica surface through the hydrolysis and condensation of TEOS catalysed by ammonia [34]. Finally, the samples were placed above the flame of a paraffin candle in a slowly reciprocating motion (one time of come-and-go per second) to form the target films.

### 2.3 Characterization

The surface morphologies of the obtained samples were observed by environmental scanning electronic microscopy (ESEM, FEI Quanta 250, USA). Water contact angles and sliding angles were measured on a contact angle system (Data Physics OCA20) at room temperature.

### 3 Results and discussion

Figure 1 shows the representative ESEM images of the surface morphology of the silicon mold and the corresponding BMG replica. For the silicon mold (Figure 1(a, b)), ESEM images clearly show ordered and square micro-pit patterns. The length and width of the micro-pit are about 20 and 20  $\mu\text{m}$ , respectively. The spacing between the neighboring micro-pits is about 9  $\mu\text{m}$ . The cross-sectional ESEM image clearly demonstrates the depth of the micro-pit is about 28–30  $\mu\text{m}$ . Utilizing the silicon micro-pit pattern as a mold, the BMG replica was successfully fabricated, exhibiting a regular array of square micro-convexes. ESEM images shown in Figure 1(c) indicate the resultant BMG displays a negative pattern of the silicon mould features.

The length, width, and spacing of the micro-pillars are about 20, 20, and 9  $\mu\text{m}$  respectively. The cross-sectional ESEM image indicates that the cavity of silicon moulds was partly filled by the metallic glass after the thermoplastic forming procession (Figure 1(d)). The filling depth of the glassy pillars is less than half of the depth of the Si micro-pit stamp. The height of the micro-pillars is 12–13  $\mu\text{m}$ . These results demonstrated the ability of BMGs to precisely replicate mould features through the direct micro-patterning of metallic glasses by the thermoplastic forming-based processing techniques. The construction of BMG surfaces with ordered micro-arrays makes it possible to fabricate multifunctional BMG materials through the further modification. Alternatively, owing to its high strength and durability, the resultant BMG pattern can even be used

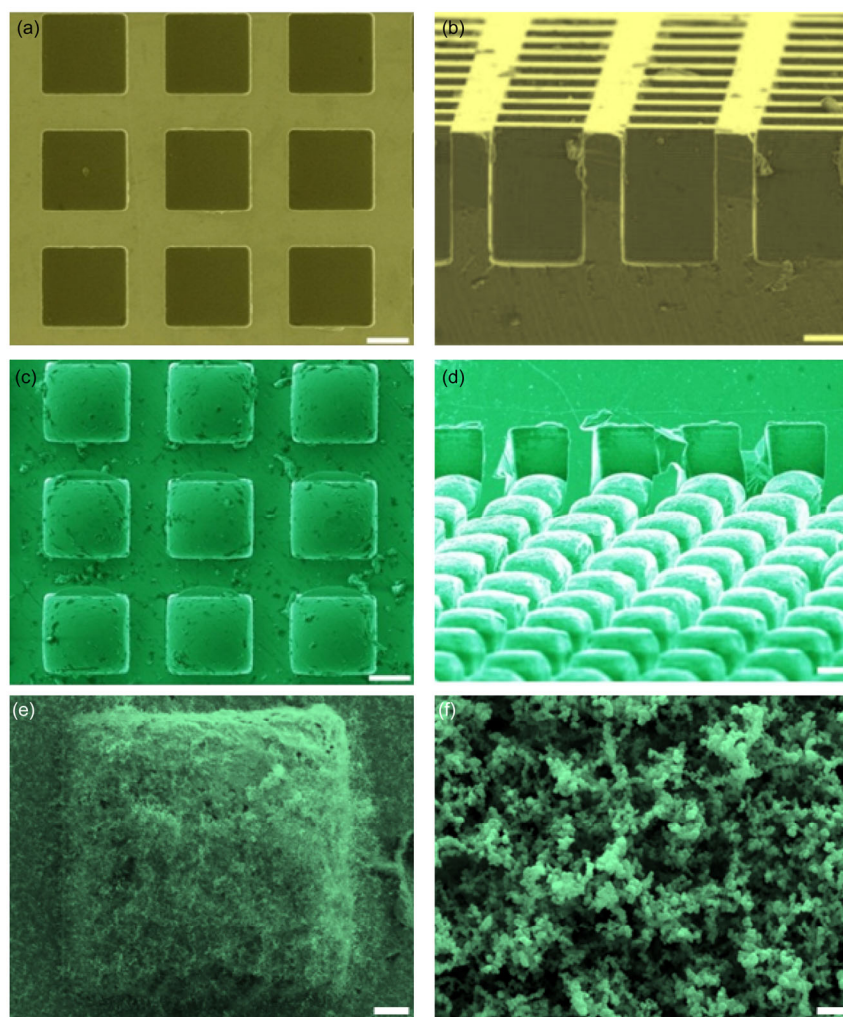


**Figure 1** ESEM images of the silicon mould surface and the resultant bulk metallic glass replica surface at different magnification. (a) A top view of the silicon stamp, exhibiting ordered and square micro-pit patterns with about 20  $\mu\text{m}$  (length) $\times$ 20  $\mu\text{m}$  (width) $\times$ 9  $\mu\text{m}$  (spacing); (b) cross-sectional ESEM image of the silicon mould, showing the depth of the micro-pit is about 28–30  $\mu\text{m}$ ; (c) a top view of the bulk metallic glass replica, showing a regular array of square micro-pillars with 20  $\mu\text{m}$  (length) $\times$ 20  $\mu\text{m}$  (width) $\times$ 9  $\mu\text{m}$  (spacing); (d) cross-sectional ESEM image of the bulk metallic glass replica with 12–13  $\mu\text{m}$  in height; (e, f) ESEM images of the bulk metallic glass replica after the  $\text{SiO}_2$ /soot deposit at different magnification. Randomly distributed nanostructures covered on the BMG micro-pillars, resulting in the micro-nanoscale hierarchical structures. The scale bars are 10  $\mu\text{m}$  (a–d), 3  $\mu\text{m}$  (e), and 500 nm (f). (color online)

as a mould for thermoplastic polymers or other metallic glasses with lower softening temperatures, which overcomes the limitations of silicon-based and metal moulds. In order to construct lotus leaf-like micro-nanoscale hierarchical structures, SiO<sub>2</sub> and soot were successively deposited on the BMG replica. ESEM images demonstrate a fractal-like network composed of randomly distributed nanostructures on BMG micro-pillar surfaces (Figure 1(e, f)). The surface structure of the resultant BMG replica in the form of microscale pillars covered by random nano-structures is quite similar to that of the natural lotus leaf with micro-papillae covered by branch-like nanostructures.

In its supercooled liquid region, the BMG exists as a high viscous liquid and the flow of the BMG is assumed as creeping flow characteristics [35]. Under these conditions, the formability of a BMG in the supercooled liquid region obeying Newtonian flow can be quantified using the Hagen-Poiseuille Equation:

$$P=32\eta Lv/d^2 \quad (1)$$

where  $P$  is the required pressure to move a liquid with viscosity ( $\eta$ ), at a velocity ( $v$ ), through a channel of thickness  $d$  and length  $L$  [3,36,37]. Hagen-Poiseuille Equation is a physical law for cylindrical molds, which presumes that the flow is fully developed in the mould. However, this law does not consider the change in pressures during the extrusion process [37]. Furthermore, in our case the shape of the mould is square (Figure 2). Therefore, further fundamental research is still necessary to investigate the quantitative relationship and to propose an effective equation to accurately describe the process using different shaped moulds.

Figure 3(a) shows an image of a water droplet on the surface of the original flat Ce-based BMG. The water contact angle is about 40°, exhibiting the intrinsic hydrophilicity of original Ce-based BMGs [38]. Even after modification with low surface energy fluoroalkylsilane, the

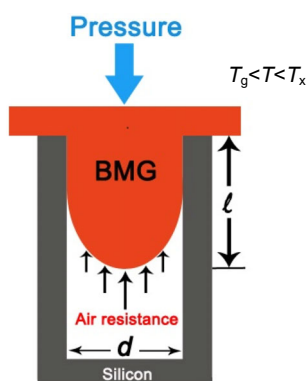


**Figure 2** Schematic diagram for the formation of the BMG micropillar with a hemispherical top in the Si mould at the temperature range between  $T_g < T < T_x$ . A square mold cavity was filled with a BMG viscous liquid, where the BMG was processed under the pressures from the external and internal. (color online)

water contact angle on the flat BMG surface is increased to about 110° (Figure 3(b)). This can be attributed to the introduction of low surface energy fluoroalkylsilane coating on the original flat BMG substrate, which increases its water repellent property. In this case, superhydrophobicity cannot be reached due to the insufficient surface roughness on the flat BMG surface. After the micro-imprinting process using the silicon mould, the resultant BMG replica with a regular array of square micro-pillars exhibited superhydrophilicity, where the water contact angle approaches 0° (Figure 3(c)). After the deposition of SiO<sub>2</sub> and soot, the case is just contrary. The water droplet with spherical shape locates on the BMG replica. The water contact angle is larger than 155°, demonstrating superhydrophobicity as observed on the lotus leaf (Figure 3(d)). It indicated that both surface roughness and surface chemical composition play an important role in the formation of superhydrophobicity.

Recently, superhydrophobic metallic glass surfaces with honeycomb micro-structures were fabricated through hot-embossing [39–41]. The resultant BMG surfaces exhibited high adhesion to water, which may be undesired for their applications in the field of self-cleaning. It has been demonstrated that micropillars with a hemispherical top were the most appropriate for the fabrication of low adhesive superhydrophobic surfaces [42,43]. In our case, in addition to hemi-spherically topped micropillars, randomly distributed nanostructures located on the BMG micro-pillars. It was found the resultant BMG replica possessed not only superhydrophobicity but a low adhesion property towards water, similar to the lotus effect found in nature. The water droplet is hardly able to stick on the BMG surface, allowing water droplets to roll off quite easily. This can be directly confirmed by the evolving contact process of a water droplet on the

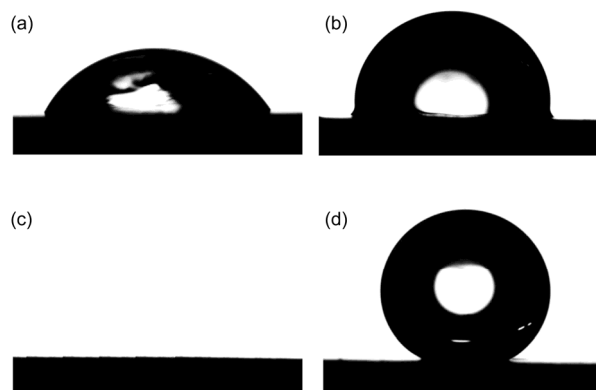


**Figure 3** (a, b) Water contact angle images of original smooth BMGs before (a) and after (b) low surface energy fluoroalkylsilane modification. After modification, the wettability of the original BMG was transformed from hydrophilicity (about 40°) to hydrophobicity (about 110°). (c, d) Water contact angle images of BMG replica with micro-pillars arrays before (c) and after (d) the deposition of SiO<sub>2</sub> and soot. After the deposition, the wettability of the BMG replica was transformed from superhydrophilicity (about 0°) to superhydrophobicity (larger than 155°).

superhydrophobic BMG surface (Figure 4). The water droplet rolled off the BMG surface quickly within a very short time (about 0.57 s) when it was tilted by about 5°. The simultaneous superhydrophobicity and a low adhesion towards water make it possible to use the BMG in the field of self-cleaning.

In nature, surface structures and surface compositions-induced special wettability has significant biological importance in living creatures. For the lotus leaf, the presence of water or dirt on its surface will affect its photosynthesis ability and then result in the leaf decomposition. Therefore, lotus leaves exhibit low-adhesive superhydrophobic self-cleaning through the evolution, arising from the cooperation of surface multiscale structures and hydrophobic epicuticular waxes [44]. Water droplets can roll freely in all directions and then pick up dirt particles on lotus leaf surfaces. In order to investigate the self-cleaning ability, the superhydrophobic BMG was contaminated with glass powder. As shown in Figure 5(a), the water droplet can't move over the original smooth BMGs contaminated with glass powder owing to the inherent hydrophilicity. However, for the resultant superhydrophobic BMGs replica, the water

droplet can adsorb the glass powder as it moved over the BMG surface from left to right (Figure 5(b)). Contaminants were efficiently removed from the BMG surface, demonstrating a lotus leaf-like self-cleaning effect as found in nature. The BMG materials with self-cleaning will strongly extend their practical engineering applications in catalysis, small-scale devices, and biomedical fields.

The wettability of solid surfaces with a liquid is governed by two factors. One is the surface chemical factor, and the other is the solid surface geometrical factor [45]. Surface geometrical structures, such as the shape, size, height, and other parameters play a critical role in surface wettability, especially to achieve surface superhydrophobicity [43,46–48]. Concerning the influence of the surface roughness on the wettability of a solid, two distinct wetting models have been proposed: the Wenzel and Cassie-Baxter models. According to the Wenzel model, the space between the protrusions on the solid surface is thoroughly filled by the liquid and both hydrophobicity and hydrophilicity can be reinforced by the roughness [49]. The Cassie-Baxter model predicts air may be trapped in the microstructures of a rough surface, resulting in a composite solid-liquid-air interface [50]. In our case, the resultant BMG replica showed multiscale structures in the form of microscale pillars with hemispherical bumps covered by randomly distributed nanostructures. Therefore, the wetting regime in this case can be described by the following equation:

$$\cos\theta^* = -1 + \phi_B(\cos\theta_Y + 1)^2 \quad (2)$$

where  $\theta^*$  is the water contact angle on a rough surface;  $\phi_B$  is the ratio of the surfaces of the spike bases over the total solid surface; and  $\theta_Y$  is the Young's angle of water on a smooth surface with identical chemical composition [42, 43,51]. Surface micropillars with a hemispherical top were proved to be the most appropriate for the fabrication of lotus-like superhydrophobic materials with low contact angle hysteresis, where air is trapped below the liquid, inducing a composite interface between the solid and the droplet and forming a discontinuous solid-liquid-air three-phase contact line [42,43]. In this case, the cooperation of

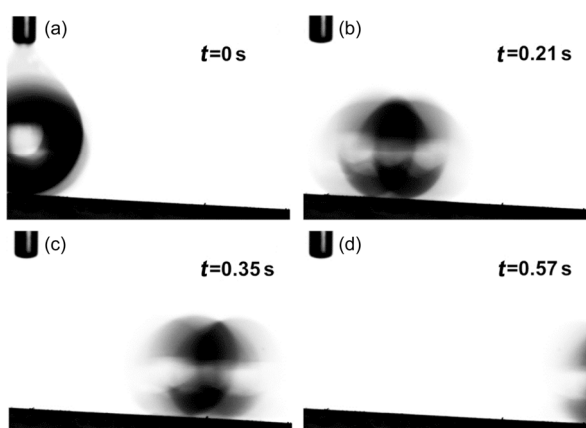


**Figure 4** The representative contact process of a water droplet (10  $\mu\text{L}$ ) on the lotus leaf-inspired superhydrophobic bulk metallic glass surface, exhibiting a low adhesion property towards water with a sliding angle less than 5°.

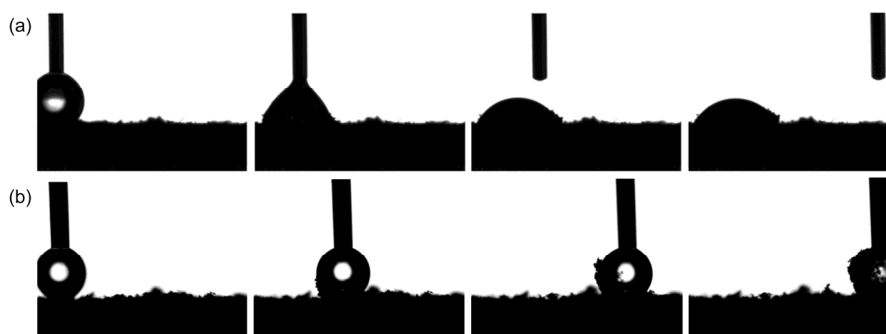


**Figure 5** Demonstration of self-cleaning ability of the original smooth BMGs (a) and superhydrophobic BMGs replica (b) through the removal of glass powder from its surface using a moving water droplet.

surface microscale pillars with a hemispherical top and the deposited SiO<sub>2</sub>/soot nanostructures on their surfaces resulted in the formation of superhydrophobicity with a low adhesion to water, exhibiting the self-cleaning property.

#### 4 Conclusions

Inspired by the self-cleaning lotus leaf with multiscale structures, multifunctional BMG surfaces have been fabricated using thermoplastic forming-based process followed by the deposition of SiO<sub>2</sub>/soot. The resultant BMG replica exhibited superhydrophobicity, a low adhesion towards water, and self-cleaning, originating from the combination of surface multiscale structures in the form of hemispherically topped micropillars covered by randomly distributed SiO<sub>2</sub>/soot nanostructures. BMGs surface with special wettability might strongly extend their practical engineering applications in catalysis, small-scale devices, and biomedical fields combined with their outstanding physical and biomedical properties. Learning from nature should give us promising inspiration to design and to fabricate advanced materials for multifunctional integration. We also expect that this method can be widely adopted for the preparation of various BMG surfaces with desirable multifunctional properties.

**Acknowledgments** This work was supported by the National Natural Science Foundation of China (21273016, 51271195), the National Basic Research Program of China (2013CB933003, 2015CB856800), the Program for New Century Excellent Talents in University, Beijing Higher Education Young Elite Teacher Project, the Fundamental Research Funds for the Central Universities, 111 project (B14009), the Key Research Program of the Chinese Academy of Sciences (KJZDEW-M01, M03).

**Conflict of interest** The authors declare that they have no conflict of interest.

- 1 Klement W, Willens RH, Duwez P. *Nature*, 1960, 187: 869–870
- 2 Wu ZW, Li MZ, Wang WH, Liu KX. *Nat Commun*, 2015, 6: 6035
- 3 Kumar G, Desai A, Schroers J. *Adv Mater*, 2011, 23: 461–476
- 4 Wang WH. *Adv Mater*, 2009, 21: 4524–4544
- 5 Wang WH. *Prog Mater Sci*, 2012, 57: 487–656
- 6 Byrne CJ, Eldrup M. *Science*, 2008, 321: 502–503
- 7 Kumar G, Tang HX, Schroers J. *Nature*, 2009, 457: 868–872
- 8 Liu YH, Wang G, Wang RJ, Zhao DQ, Pan MX, Wang WH. *Science*, 2007, 315: 1385–1388
- 9 Sarac B, Ketkaew J, Popnoe DO, Schroers J. *Adv Funct Mater*, 2012, 22: 3161–3169
- 10 Zhang B, Zhao DQ, Pan MX, Wang WH, Greer AL. *Phys Rev Lett*, 2005, 94: 205502
- 11 Liu K, Jiang L. *ACS Nano*, 2011, 5: 6786–6790
- 12 Aizenberg J, Fratzl P. *Adv Mater*, 2009, 21: 387–388
- 13 Liu K, Jiang L. *Nano Today*, 2011, 6: 155–175
- 14 Chen PY, McKittrick J, Meyers MA. *Prog Mater Sci*, 2012, 57: 1492–1704
- 15 Liu KS, Cao MY, Fujishima A, Jiang L. *Chem Rev*, 2014, 114: 10044–10094
- 16 Bellanger H, Darmanin T, de Givenchy ET, Guittard F. *Chem Rev*, 2014, 114: 2694–2716
- 17 Liu K, Yao X, Jiang L. *Chem Soc Rev*, 2010, 39: 3240–3255
- 18 Zheng YM, Gao XF, Jiang L. *Soft Matter*, 2007, 3: 178–182
- 19 Gao XF, Jiang L. *Nature*, 2004, 432: 36
- 20 Liu K, Du J, Wu J, Jiang L. *Nanoscale*, 2012, 4: 768–772
- 21 Zheng YM, Bai H, Huang ZB, Tian XL, Nie FQ, Zhao Y, Zhai J, Jiang L. *Nature*, 2010, 463: 640–643
- 22 Parker AR, Lawrence CR. *Nature*, 2001, 414: 33–34
- 23 Yang S, Du JX, Cao MY, Yao X, Ju J, Jin X, Su B, Liu KS, Jiang L. *Angew Chem Int Ed*, 2015, 54: 4792–4795
- 24 Gao SJ, Shi Z, Zhang WB, Zhang F, Lin J. *ACS Nano*, 2014, 8: 6344–6352
- 25 Sun TL, Qing GY, Su BL, Jiang L. *Chem Soc Rev*, 2011, 40: 2909–2921
- 26 Liu K, Jiang L. *Nanoscale*, 2011, 3: 825–838
- 27 Sun TL, Qing GY. *Adv Mater*, 2011, 23: H57–H77
- 28 Yao X, Song YL, Jiang L. *Adv Mater*, 2011, 23: 719–734
- 29 Bhushan B. *Langmuir*, 2012, 28: 1698–1714
- 30 Zhao H, Law KY. *ACS Appl Mater Inter*, 2012, 4: 4288–4295
- 31 Zhang WB, Zhu YZ, Liu X, Wang D, Li JY, Jiang L, Jin J. *Angew Chem Int Ed*, 2014, 53: 856–860
- 32 Zhang F, Zhang WB, Shi Z, Wang D, Jin J, Jiang L. *Adv Mater*, 2013, 25: 4192–4198
- 33 Zhang B, Pan MX, Zhao DQ, Wang WH. *Appl Phys Lett*, 2004, 85: 61–63
- 34 Stöber W, Fink A, Bohn E. *J Colloid Interf Sci*, 1968, 26: 62–69
- 35 Schroers J. *Jom-US*, 2005, 57: 35–39
- 36 Schroers J. *Adv Mater*, 2010, 22: 1566–1597
- 37 Chiu HM, Kumar G, Blawdziewicz J, Schroers J. *Scr Mater*, 2009, 61: 28–31
- 38 Liu K, Li Z, Wang W, Jiang L. *Appl Phys Lett*, 2011, 99: 261905
- 39 Xia T, Li N, Wu Y, Liu L. *Appl Phys Lett*, 2012, 101: 081601
- 40 Li N, Xia T, Heng LP, Liu L. *Appl Phys Lett*, 2013, 102: 251603
- 41 Ma J, Zhang XY, Wang DP, Zhao DQ, Ding DW, Liu K, Wang WH. *Appl Phys Lett*, 2014, 104: 173701
- 42 Nosonovsky M, Bhushan B. *Microsyst Technol*, 2005, 11: 535–549
- 43 Bico J, Marzolin C, Quéré D. *Europhys Lett*, 1999, 47: 220–226
- 44 Liu K, Jiang L. *Annu Rev Mater Res*, 2012, 42: 231–263
- 45 Shibuichi S, Onda T, Satoh N, Tsujii K. *J Phys Chem*, 1996, 100: 19512–19517
- 46 Nosonovsky M. *Langmuir*, 2007, 23: 3157–3161
- 47 Jin X, Yang S, Li Z, Liu K, Jiang L. *Sci China Chem*, 2012, 55: 2327–2333
- 48 Ahuja A, Taylor JA, Lifton V, Sidorenko AA, Salamon TR, Lobaton EJ, Kolodner P, Krupenkin TN. *Langmuir*, 2008, 24: 9–14
- 49 Wenzel RN. *Ind Eng Chem*, 1936, 28: 988–994
- 50 Cassie A, Baxter S. *Trans Faraday Soc*, 1944, 40: 546–551
- 51 Martinez E, Seunarine K, Morgan H, Gadegaard N, Wilkinson CDW, Riehle MO. *Nano Lett*, 2005, 5: 2097–2103